HHS Public Access

Author manuscript

Circ Arrhythm Electrophysiol. Author manuscript; available in PMC 2017 April 01.

Published in final edited form as:

Circ Arrhythm Electrophysiol. 2016 April ; 9(4): . doi:10.1161/CIRCEP.115.003520.

Quantification of Left Ventricular Function with Premature Ventricular Complexes Reveals Variable Hemodynamics

Francisco Contijoch, PhD[1], **Kelly Rogers, BS**[2], **Hannah Rears**[3], **Mohammed Shahid, MS**[3], **Peter Kellman, PhD**[4], **Joseph Gorman III, MD**[5], **Robert C. Gorman, MD**[5], **Paul Yushkevich, PhD**[3], **Erica S. Zado, PA-C**[2], **Gregory E. Supple, MD**[2], **Francis E. Marchlinski, MD**[2], **Walter R.T. Witschey, PhD**[3], and **Yuchi Han, MD**[2]

1

2

3

4

5

Abstract

Background—Premature ventricular complexes (PVC) are prevalent in the general population and are sometimes associated with reduced ventricular function. Current echocardiographic and cardiovascular magnetic resonance imaging (CMR) techniques do not adequately address the effect of PVCs on left ventricular function.

Methods and Results—Fifteen subjects with a history of frequent PVCs undergoing CMR had real-time slice volume quantification performed using a 2D real-time CMR imaging technique. Synchronization of 2D real-time imaging with patient ECG allowed for different beats to be categorized by the loading beat RR-duration and beat RR-duration. For each beat type, global volumes were quantified via summation over all slices covering the entire ventricle. Different patterns of ectopy including isolated PVCs, bigeminy, trigeminy, and interpolated PVCs were observed. Global functional measurement of the different beat types based on timing demonstrated differences in preload, stroke volume, and ejection fraction. An average of hemodynamic function was quantified for each subject depending on the frequency of each observed beat type.

Conclusions—Application of real-time CMR imaging in patients with PVCs revealed differential contribution of PVCs to hemodynamics.

Keywords

premature ventricular complexes; real-time imaging; arrhythmias; cardiac function

Correspondence: Francisco Contijoch, PhD, Department of Bioengineering, University of Pennsylvania, 3400 Civic Center Blvd, Bldg 421, 7th Floor, Rm 103, Philadelphia, PA 19036, Tel: 215-746-4048, Fax: 215-746-2375, fcont@seas.upenn.edu.

Conflict of Interest Disclosures: None

Introduction

Premature ventricular complexes (PVCs) are early electrical depolarizations originating in the ventricular myocardium, which can disrupt the coordinated electrical depolarization and mechanical contraction of the heart. Idiopathic PVCs may create variable symptoms and may cause a cardiomyopathy. Clinically, PVC-induced cardiomyopathy remains a diagnosis of exclusion and conventional imaging is often employed to rule out underlying disease[1].

Accurate assessments of left ventricular (LV) function using conventional multi-shot cardiovascular magnetic resonance (CMR) acquisitions are hindered by the presence of frequent PVCs due to the irregularly irregular rhythm. In conventional multi-shot 2D CMR, data for a single slice is acquired over multiple cardiac cycles and arrhythmias can lead to incorrect combination of data causing considerable image corruption[2]. Retrospective ECG-gated acquisitions can employ arrhythmia rejection to eliminate corruption due to ectopic beats. However, this approach discards data from ectopic contractions, markedly prolongs scan time during frequent PVCs, and can result in respiratory motion artifacts due to unachievable breath-hold duration. Prospective ECG-gated acquisitions can also be utilized in patients with arrhythmias. If an arrhythmia is very regular, the acquisition window can be prolonged to acquire several beats after each QRS. Unfortunately, this approach is easily corrupted by any irregularity in the rhythm pattern and also markedly prolongs the scan time, making it sensitive to respiratory motion artifacts.

Single-shot (real-time) 2D CMR eliminates the need for combination of data acquired from multiple heartbeats and allows for observation of each cardiac contraction in a 2D slice[3]. The decreased spatial and temporal resolution associated with conventional real-time imaging has previously led to a loss of slice volume accuracy[4]. However, by combining non-Cartesian data acquisition, iterative image reconstruction, and semi-automated image processing, high spatial and temporal resolution real-time CMR images can be obtained and led to accurate measurement of 2D slice volume in a per-beat fashion[5,6].

In this work, we combine a previously-validated 2D real-time imaging technique with synchronous ECG recording, which allows for identification of different beat types based on RR intervals and the measurement of global LV volume via summation of 2D slice data covering the entire heart for each beat type.

Methods

Patient Population

The prospective study was approved by the Institutional Review Board at the University of Pennsylvania and all subjects (n=15, 47.7 ± 23.6 years old and 46.7% male) gave written informed consent. PVC burden was quantified via synchronously recorded ECG during CMR acquisition. Two subjects had no PVCs during the CMR exam despite a history of frequent PVCs. 13 patients had PVCs during real-time CMR (burden 25 ± 14%, range 4-50%) and they demonstrated a range of arrhythmic patterns including bigeminy, trigeminy, and interpolated PVCs. Two of the 13 subjects (Subject 5 and 6) were imaged

twice. Subject 5 was imaged pre and post PVC ablation and Subject 6 had two different PVC burdens and ectopic patterns during two imaging sessions.

CMR Acquisition

CMR was performed on a 1.5 T imaging system (Avanto, Siemens Healthcare, Erlangen, Germany) equipped with nominal 40 mT/m magnetic field gradients, body RF transmit and a 32-channel, anterior and posterior RF receiver array.

Real-time data was obtained using a 2D, multi-slice, free-breathing balanced steady-state free precession (bSSFP) sequence with a golden-angle radial trajectory with the following imaging parameters, TE = 1.4 ms, TR = 2.8 ms, number of radial k-space data = 128, FOV = 220 mm - 300 mm, pixel size = 1.72 – 2.34 × 1.72 – 2.34 mm, bandwidth = 1000-1221 Hz/pixel, slice thickness = 8 mm, slice spacing = 10 mm, and k-space sampling according to the golden-angle Φ=111.25°. 2D imaging was performed at short axis slice positions covering the entire left ventricle. 6000 - 8000 radial projections (16 - 22 seconds) per slice were acquired.

Image Reconstruction and Slice Volume Quantification

The real-time image reconstruction and slice volume quantification methods have recently been validated in animals as well as in clinical patients[5,6]. Briefly, image reconstruction was performed using a non-Cartesian SENSE algorithm in open-source software with 34 radial projections per image (image exposure time = 95.2 ms) and maximal view sharing (frame rate = 357 fps)[7-9]. Quantification of real-time images was performed through user-initialized active contour segmentation which has been shown to provide slice volume values comparable to manual segmentation using clinical tools[6]. Papillary muscles were excluded from the segmentation using the feature image and manual correction. The basal slice was determined by identification of the slice with mitral valve annular plane at end-systole. LV slice volume was quantified from segmented data using the pixel size and slice thickness.

ECG Recording and Synchronization

Electrocardiograms (ECGs) recorded in a magnetic field are distorted by the magnetohemodynamic effect, which limits the interpretability of the 3-lead ECG as compared with a 12-lead ECG outside of the magnet[10]. However, due to the need for ECG gating in cine CMR, robust 3-lead (ECG) acquisition, filtering, and real-time display are standard features of clinical CMR scanners. For this work, we implemented a logging algorithm to capture the ECG signal acquired during CMR. This results in synchronization between the ECG signal, real-time CMR image frames, and derived slice volume quantification as shown in Figure 1. The ECG distortion did not hinder detection of QRS peaks and allowed for quantification of RR durations[11]. Although QRS morphology is distorted by the magnetic field, the distortion is consistent across the same PVC beat type, which allowed for identification of each PVC beat type in all patients as well as exclusion of premature atrial contractions. ECG recording was continuous and synchronous during the imaging of the entire short axis of the LV. PVC burden was quantified as the percentage of total beats during the scanning session.

Categorization of Beats

After detection of the R-wave of the QRS complex via Pan-Tompkins algorithm implemented in Matlab (Mathworks, Natick MA), different beats were identified and categorized based on two measured RR-durations[11]. As shown in Figure 2, plotting the RR-duration of the prior (loading) beat RR_{i-1} versus RR-duration of the current beat RR_i allowed for clustering of different beats. Specifically, in sinus rhythm, a single cluster is observed (Figure 2A). In patients with occasional PVCs, the clustering acts as robust arrhythmia rejection as only the sinus rhythm beats are sampled across all slices (Figure 2B). Multiple clusters indicate the presence of distinct beat types and when a cluster is observed across all slice locations, global volume quantification of that beat type can be performed (Figure 2C).

For each ectopic contraction, there is a potential for four distinct beat types to be observed via the 2D clustering of RR_{i-1} and RR_i. First, during normal sinus rhythm, the RR_{i-1} of the preceding beat and RR_i of the current beat are similar and thus forms a sinus-sinus beat. Second, when a PVC occurs, the sinus beat preceding the PVC is characterized by a normal RR_{i-1} and is followed by a short RR_i due to the premature depolarization. This is termed an interrupted sinus beat. Third, the PVC beat is characterized by a short RR_{i-1} followed by a long RR_i. Finally, the beat following a PVC is characterized by a long RR_{i-1} followed by a normal RR_i, which is the post PVC-sinus beat. In any particular patient, not all four beat types may be present or distinguishable using this 2D clustering method with RR_{i-1} and RR_i. For example, in regular trigeminy, the sinus-sinus pattern does not occur. Similarly in bigeminy, only a PVC beat and a post-PVC sinus are observed, resulting in only two patterns: short RR_{i-1} - long RR_i and long RR_{i-1} - short RR_i. Even in irregular ectopic patterns where all four beat types occur, identification of these beat types based on two RR-durations may result in some beat types being classified together due to negligible differences in RR_{i-1} and RR_i.

Global Volume Estimation

For each beat type, global volume estimates were obtained by summation of slice volumes obtained across the LV (Figure 3). To account for small variations in RR-duration, non-linear beat duration normalization was performed prior to summation[12]. Global volume over time was obtained only in beat types that were observed at all LV slice locations.

Global volume estimates made during PVCs are illustrated in Figure 4. Subject 6 has a regular bigeminy pattern (Figure 4A) and two beat types (clusters) are identified in Figure 4B. Panels C and D illustrate the close agreement in ECG morphology across the observed beats. The global volume over time for each beat type is obtained by summation of slice volumes over time.

Quantification of Beat-by-Beat Function

Global maximum volume (V_{max}) (end diastolic volume (EDV) in sinus beats, loading volume in PVC beats), global minimum volume (V_{min}) (end systolic volume (ESV) in sinus beats, smallest volume in the PVC beats), SV ($V_{max} - V_{min}$ for the beat), and EF (SV/V_{max}) were obtained for each observed beat type. The prevalence of each type was used to obtain a

temporally averaged estimate of function. The prevalence of each type was calculated as the percentage of beats identified in that beat type relative to the number of beats used for global volume estimation of all beat types. LVEF obtained from clinically performed echocardiography exams were compared to MRI-derived values when available.

Evaluation of PVC Function Across Subjects

To understand the relationship of PVC timing to stroke volume produced by the PVCs, we plotted the SV of PVC contractions (normalized to the SV observed in sinus or interrupted sins beats in that subject) versus loading duration of the PVC (normalized by the loading duration of sinus beats in the same subject = $RR_{i-1,PVC}$ / $RR_{i-1,Sinus}$). In the setting of bigeminy, the post-PVC contraction is used for normalization.

Intra- and Inter-Observer Variability

The variation in the proposed approach stems mainly from the reproducibility of semi-automated segmentation of the individual LV slices. To quantify this variability, a mid-ventricular slice was re-segmented by the same observer as well as by a second observer for each imaging study (n=17), The slice EDV and ESV were estimated from 5 consecutive heartbeats as the mean maximum and mean minimum slice volume, respectively.

Statistical Analysis

Non-parametric Wilcoxon rank sum test ($p<0.05$) was used to detect significant differences in the comparison of PVC burden between patients with normal and abnormal LV EF as well as differences between echo- and MRI-derived EF. Skewness and kurtosis test for normality was performed for SV and EF after normalizing the volumes to each subject's sinus or interrupted sinus beat. Repeated measures ANOVA were performed to evaluate differences in SV and EF amongst different beat types (sinus, interrupted sinus, post-PVC sinus, and PVC). Intra- and inter-observer reliability was quantified by coefficient of variation and Pearson correlation coefficient. Statistical analyses were performed using Stata 13 (StataCorp, College Station, TX).

Results

Sinus Rhythm and Low Frequency of PVCs

In 5 subjects (Table 1, Patients 1-4 and 5 Post Ablation), only one beat type (sinus rhythm) was observed across all slice locations and thus one mode of ventricular volume and function was quantified (Figure 3). These subjects were in sinus rhythm despite having a history of frequent PVCs (Patients 1 and 2) or had infrequent PVCs (4%, 7% and 8% PVC burden (Patient 3, 4, and 5 post ablation) during the imaging session. These PVCs were not observed at all slice positions and could not be quantified with data obtained during the scanning session.

High Frequency of PVCs in Different Ectopic Patterns

The remaining 10 subjects had PVCs that were observed in all slice locations during imaging (13 - 50%). The PVC burden calculated based on the ECG differs from that

prevalence of beat-types due to changes in rhythms (for example, sinus to trigeminy or bigeminy to trigeminy). As a result, the beat types described Table 1 may not contain all of the cardiac contractions; hence the sum of beat frequencies is less than 100%.

Subject 6 was imaged twice and was in regular bigeminy during the first real-time CMR. As a result, two beat types were observed (Figure 4). The lower EF of the PVC was a result of less effective contraction with similar loading volume as the post-PVC sinus contraction, leading to a higher V_{min}. During the second imaging session, the same subject had frequent PVCs (40%) without a regular pattern. The PVCs were less effective toward cardiac output than the PVCs in bigeminy and contributed half of the SV compared to sinus beats (23.5 ml vs. 52.9 ml). Despite the difference in ectopic patterns at different time points, the temporally averaged EFs were similar (48.7% vs. 50.1%) during the two imaging sessions.

Subject 7 was in regular trigeminy during the real-time CMR, which resulted in 3 beat clusters (Figure 5). In addition to the PVC, the 2D RR-duration plot allowed for the interrupted sinus cluster to be quantified separately from the post-PVC sinus and sinus-sinus cluster, shown in Figure 5C and 5D. V_{min} associated with the post-PVC sinus was smaller than the interrupted sinus (38.7 ml vs. 65.8 ml), which resulted in a higher calculated EF (69.5 vs. 50.5%). The PVCs (Figure 5E) in this pattern had a small stroke volume (9.6 ml). As a result, this patient demonstrated two contractions (interrupted sinus and post-PVC sinus) that produced high stroke volumes and one contraction (PVC) that produced very low stroke volume.

Subject 8 had interpolated PVCs during the image acquisition (Figure 6), which resulted in a unique pattern not described above. During interpolated PVCs, the PVC is an ‘extra’ depolarization in between sinus activity, which does not change the sinus P wave to P wave duration: in this case, there are two short RR intervals occurring sequentially. The loading volume for the post-PVC sinus contraction (94.4 mL) decreased relative to normal sinus beats (126.8 mL). The post-PVC contraction resulted in a decrease in EF (34.6 vs. 42.6 %). Furthermore, the PVC did not result in substantial SV (14.0 mL). As a result, interpolated PVCs resulted in a decreased SV not only in the PVC beat but also in the post-PVC beats.

Subjects 9-15 and subject 5 prior to ablation had a variety of patterns including periods of bigeminy and trigeminy, as well as PVCs late in diastole. The different arrhythmia patterns resulted in different number of beat types being observed, which are also quantified in Table 1. After normalizing the SV and EF to each subject’s sinus or interrupted sinus beats, both variables were tested and found to be normally distributed. There were statistically significant differences in SV ($p < 0.0001$) and EF ($p < 0.0001$) between PVC and non-PVC beats. Differences between non-PVC beats (sinus, interrupted sinus, and post-PVC sinus) were not significant (SV $p = 0.30$ and EF p-value = 0.51).

In 5 subjects with clinically performed cardiac echocardiograms preceding their MRI examination. The echo-derived EF was assessed using the biplane method and is shown in Table 1. When compared to non-PVC contractions, the values show close agreement (p-value = 0.84, $R^2 = 0.986$, CoV = 5.8%)

PVC SV and Timing

To further understand the relationship of PVC timing to stroke volume produced by the PVCs, we plotted the SV of the PVC (normalized to the SV observed during sinus contractions in that subject) versus loading duration of PVC (normalized by the loading duration of sinus beats in the same subject) as shown in Figure 7. The SV of PVC correlated poorly to the timing in the cardiac cycle (linear fit: slope = 0.27, y-intercept = 23.6, R^2 = 0.03, p-value = 0.552).

Inter- and Intra-observer Reproducibility

The reproducibility results are shown in Table 2. Pearson coefficients values were high for both cardiac phases as well as intra- and inter-observer measurements.

Discussion

In this work, we have demonstrated a technique, which combines a 2D real-time MR imaging technique and simultaneous ECG logging to quantify ventricular volumes. This technique allowed us to characterize different PVCs by volume and compare them to other beats in the same subject, which revealed differential stroke volume and contribution to cardiac output. In subjects with similar PVC frequencies, the hemodynamic impact of PVCs occurring in different patterns can be significantly different. In addition, we have reported that PVCs can potentially lower subsequent sinus loading volume rather than augmenting it.

Assessment of LV Function

There is currently no standard non-invasive method to assess the volumes and functions of PVCs in addition to sinus contractions. In echocardiography, which has been used as the standard in evaluating patients with suspected PVC-induced cardiomyopathy, PVCs are ignored in situations other than bigeminy (in which case sinus beats and PVC beats are averaged)[13]. Our method correlates closely with echocardiography in assessing the non-PVC beats.

Amongst the 15 subjects, if we consider the LV function to be represented by the “normal depolarization” beats including sinus, interrupted sinus, and post-PVC sinus beats, then subjects 6, 7, 9, 10, 13, and 15 would have “normal” function. Their burden of PVCs measured by PVC frequency was not significantly different from the remaining subjects with “abnormal” LVEF (Wilcoxon rank test, p=0.23). If we instead consider the average EF of all beats as the representation of LV function, only subjects 9 and 10 would have “normal” function. These two subjects had high burdens of PVCs (35% and 33%) but also had the 2 latest occurring PVCs (675 ms and 766 ms after the previous QRS, respectively) and therefore these PVCs produced stroke volumes that were similar to sinus beats, which limited the hemodynamic impact of the PVCs. The PVC contribution to hemodynamics coupled with PVC frequency may be more important than frequency alone. For example, subject 6 had a PVC prevalence of 40-50%, but all the PVCs produced considerable stroke volume while subject 7 had a prevalence of 33% with PVCs that produced little stroke volume. It is believed that PVC-induced cardiomyopathy develops in a time-dependent

fashion where the cumulative burden over time may play an important role[14]. Future longitudinal work examining the impact of hemodynamics as well as frequency is needed.

It has long been recognized that PVC burden is only one of the many factors contributing to impairment of LV systolic function in PVC-induced cardiomyopathy. PVC interpolation has been identified as an additional independent predictor but the hemodynamic mechanism has not been elucidated[15]. In one subject with interpolated PVCs, we observed the stroke volumes of both the PVC and the post-PVC contraction being impaired. This has not been previously reported and the implication of this finding would need to be investigated in a larger sample.

Previously, it has been reported that PVCs with coupling intervals ≤ 600 ms have a lower mean LVEF[16] but a recent study suggests a longer coupling interval leads to more dyssynchronous contraction[17]. Our study has shown a poor correlation between the coupling intervals of the PVC and the stroke volume produced. This might be due to the heterogeneity of our subject population including key factors such as the origin of the PVC, degree of dyssynchrony associated with the PVC contraction, and degree of underlying cardiomyopathy. Future studies are needed to further examine this relationship using this technique.

Clinical Relevance of the Technique

A variety of mechanisms have been proposed for PVC-induced cardiomyopathy including hemodynamic impairment, alterations in heart rate, vascular autonomic dysregulation, increased oxygen consumption, ventricular dyssynchrony, tachycardia-induced cardiomyopathy, or alterations in calcium and ionic currents[1,18], but it remains unclear what are the underlying causes of PVC-induced cardiomyopathy. Animal pacing models have also been utilized to better understand the myocardial dysfunction caused by PVCs[19,20]. These models have found changes in global LV dimensions and function after 2 - 4 weeks of pacing with bigeminy that were programmed with a short coupling interval. These animal models suggest that PVCs can cause a reversible cardiomyopathy in structurally normal hearts but the question of what differentiates benign PVCs and myopathy-causing PVCs remains unanswered.

Our approach may allow us to understand the hemodynamic features of PVCs better as the patients with the same frequencies might have very different hemodynamic profile of the PVCs. In addition, this technique may allow for improved patient selection for PVC ablations as eliminating low stroke volume PVCs might be more beneficial. Lastly, some patients with frequent PVCs and preserved EF may have a subclinical cardiomyopathy as demonstrated by abnormal radial strain[21], which has been recently corroborated in animal models[22]. Our approach may provide another means to identify subclinical cardiomyopathy, which might lead to earlier initiation of care and avoid the development of an overt cardiomyopathy.

To understand the hemodynamics of other arrhythmias such as atrial fibrillation, pacing models of otherwise healthy, instrumented animals has been previously developed[23-26]. Our

technique allows for evaluation of patients without the need for instrumentation as the ECG system and the imaging can be utilized to obtain both timing and hemodynamic information.

We only observed 30% of subjects who had increased (> 5%) EF after ectopic contractions while earlier work describes substantial post-extrasystolic potentiation. This discrepancy may be due to different patient population or measurement techniques.

Advantages over Current Techniques

The 2D real-time imaging method we utilized combines non-Cartesian k-space sampling and an iterative SENSE-based image reconstruction technique to improve the image quality (by reducing undersampling artifacts) and spatiotemporal resolution when compared to conventional real-time acquisitions. This allows for accurate estimation of slice and global volumes in sinus rhythm patients, when compared to standard cine acquisitions[5,6].

In the patients with infrequent PVCs, our approach provided arrhythmia rejection similar to clinical CMR acquisitions where only the predominant contraction mode was quantified. However, our approach is more robust as conventional arrhythmia rejection can fail in several ways. First, conventional arrhythmia rejection utilizes the RR-duration to categorize beats in real-time and may have variable success depending on the ectopic morphology and frequency. Second, if the RR-duration acceptance window is too small, a high rejection rate will lead to prolonged breathholds and the potential for respiratory motion corruption. Third, not all PVCs may be reliably detected by the vector ECG since depolarizations can sometimes resemble a T-wave. Using the real-time imaging technique, our approach is not sensitive to any of these failure modes.

Limitations

First, the entire heart is acquired with a slice-by-slice 2D real-time imaging technique. In patients with infrequent PVCs, PVCs might not occur at all slice positions, which limits the quantification of rare PVCs. In these instances, quantitative values are similar to those obtained using conventional cine CMR with arrhythmia rejection. Longer scans in these patients could allow for analysis of these infrequent PVCs. Furthermore, patients with multiple PVC morphologies (multiple coupling intervals) result in a higher number of ‘clusters’ and will require prolonged scans to capture all of the different beat morphologies.

A second limitation of this study is the potential impact of respiratory motion on measured cardiac function. We performed the real-time acquisition during free respiration to minimize the overall acquisition time. We did not use a respiratory window since it would reduce the number of observed beats and would compromise our ability to observe multiple beat types across slice locations. However, the potential effect of respiratory motion is likely small because large variations were not present in the slice volume curves (as shown in Figures 3-6). In addition, recent publications indicate that the effect of respiratory position on LV volume quantification is negligible, potentially due to a predominant in-plane as opposed to through-plane motion[27]. However, changes in intrathoracic pressure will affect cardiac loading and therefore, imaging during breathholds or selection of images based on respiratory motion could be employed in future studies to minimize this effect.

A third limitation of this approach is that our approach may combine data acquired from different PVCs beats, which occur with similar coupling intervals and PVC duration. Additional refinements to the technique are necessary to sub-divide these clusters into unique PVC types.

Additionally, our approach does not include retrospective reconstruction of motion corrected data, compressed sensing reconstructions, or low-rank image reconstruction, which have been recently proposed to further improve spatiotemporal resolution and image quality[28-31]. These techniques are complementary to the method described here and combination of those methods with this approach may allow further acceleration and improved image quality.

Conclusions

We have presented a novel CMR-based method to assess LV function including PVCs in subjects with ventricular ectopy, which provides volumetric assessment of multiple beat types. This method revealed that different ectopic patterns might contribute differently to hemodynamics. Our findings allowed for accurate interrogation of the LV function during PVCs in each individual patient and may provide new insight into PVC-induced cardiomyopathy and symptoms associated with PVCs.

Acknowledgments

Funding Sources: NIH Support: F31-HL120580, R00-HL108157, R01-EB014346, R01-HL103723, R01-HL63954, T32-HL007954, T32-EB009384. Cardiovascular Medical Research and Education Fund (Philadelphia, PA).

References

1. Cha Y-M, Lee GK, Klarich KW, Grogan M. Premature ventricular contraction-induced cardiomyopathy: a treatable condition. Circ Arrhythm Electrophysiol. 2012; 5:229–236. [PubMed: 22334430]
2. Chia J, Fischer S. Performance of QRS detection for cardiac magnetic resonance imaging with a novel vectorcardiographic triggering method. J Magn Reson Imaging. 2000; 12:678–688. [PubMed: 11050637]
3. Kühl HP, Spuentrup E, Wall A, Franke A. Assessment of Myocardial Function with Interactive Non–Breath-hold Real-time MR Imaging: Comparison with Echocardiography and Breath-hold Cine MR Imaging. Radiology. 2004; 231:198–207. [PubMed: 14990805]
4. Bauer R, Radtke I, Block KT, Larson MC, Kerl JM, Hammerstingl R, Graf TG, Vogl TJ, Zhang S. True real-time cardiac MRI in free breathing without ECG synchronization using a novel sequence with radial k-space sampling and balanced SSFP contrast mode. Int J Cardiovasc Imaging. 2013; 29:1059–1067. [PubMed: 23334191]
5. Witschey WRT, Contijoch F, McGarvey JR, Ferrari VA, Hansen MS, Lee ME, Takebayashi S, Aoki C, Chirinos JA, Yushkevich PA, Gorman JH III, Pilla JJ, Gorman RC, Gorman JH, Pilla JJ, Gorman RC. Real-Time Magnetic Resonance Imaging Technique for Determining Left Ventricle Pressure-Volume Loops. Ann Thorac Surg. 2014; 97:1597–1603. [PubMed: 24629301]
6. Contijoch F, Witschey WR, Rogers K, Rears H, Hansen MS, Yushkevich PA, Gorman JH, Gorman RC, Han Y. User-Initialized Active Contour Segmentation and Golden-angle Real-Time Cardiac MRI Enable Accurate Assessment of LV Function in Patients with Sinus Rhythm and Arrhythmias. J Cardiovasc Magn Reson. 2015; 17:37. doi: 10.1186/s12968-015-0146-9. [PubMed: 25994390]
7. Pruessmann KP, Weiger M, Börnert P, Boesiger P. Advances in sensitivity encoding with arbitrary k-space trajectories. Magn Reson Med. 2001; 46:638–651. [PubMed: 11590639]

8. Sorensen T, Atkinson D. Real-time reconstruction of sensitivity encoded radial magnetic resonance imaging using a graphics processing unit. IEEE Trans Med Imaging. 2009; 28:1974–1985. [PubMed: 19628452]
9. Hansen MS, Sorensen TS, Sørensen TS. Gadgetron: an open source framework for medical image reconstruction. Magn Reson Med. 2013; 69:1768–1776. [PubMed: 22791598]
10. Dimick RN, Hedlund LW, Herfkens RJ, Fram EK, Utz J. Optimizing electrocardiograph electrode placement for cardiac-gated magnetic resonance imaging. Invest Radiol. 1987; 22:17–22. [PubMed: 3818232]
11. Pan J, Tompkins WJ. A real-time QRS detection algorithm. IEEE Trans Biomed Eng. 1985; 32:230–236. [PubMed: 3997178]
12. Bacharach S, Bonow R, Green M. Comparison of fixed and variable temporal resolution methods for creating gated cardiac blood-pool image sequences. J Nucl Med. 1990; 31:38–42. [PubMed: 2295938]
13. Del Carpio Munoz F, Syed FF, Noheria A, Cha Y-M, Friedman P a. Hammill SC, Munger TM, Venkatachalam KL, Shen WK, Packer DL, Asirvatham SJ. Characteristics of premature ventricular complexes as correlates of reduced left ventricular systolic function: Study of the burden, duration, coupling interval, morphology and site of origin of PVCs. J Cardiovasc Electrophysiol. 2011; 22:791–798. [PubMed: 21332870]
14. Yarlagadda RK, Iwai S, Stein KM, Markowitz SM, Shah BK, Cheung JW, Tan V, Lerman BB, Mittal S. Reversal of cardiomyopathy in patients with repetitive monomorphic ventricular ectopy originating from the right ventricular outflow tract. Circulation. 2005; 112:1092–1097. [PubMed: 16103234]
15. Olgun H, Yokokawa M, Baman T, Kim HM, Armstrong W, Good E, Chugh A, Pelosi F, Crawford T, Oral H, Morady F, Bogun F. The role of interpolation in PVC-induced cardiomyopathy. Heart Rhythm. 2011; 8:1046–1049. [PubMed: 21376837]
16. Sun Y, Blom N a, Yu Y, Ma P, Wang Y, Han X, Swenne C a. Van Der Wall EE. The influence of premature ventricular contractions on left ventricular function in asymptomatic children without structural heart disease: An echocardiographic evaluation. Int J Cardiovasc Imaging. 2003; 19:295–299. [PubMed: 14598897]
17. Potfay J, Kaszala K, Tan AY, Sima AP, Gorcsan J, Ellenbogen KA, Huizar JF. Abnormal Left Ventricular Mechanics of Ventricular Ectopic Beats: Insights into Origin and Coupling Interval in Premature Ventricular Contraction-Induced Cardiomyopathy. Circ Arrhythmia Electrophysiol. 2015; 8:1194–1200.
18. Wang Y, Eltit JM, Kaszala K, Tan A, Jiang M, Zhang M, Tseng G-N, Huizar JF. Cellular Mechanism of Premature Ventricular Contraction-Induced Cardiomyopathy. Heart Rhythm. 2014; 11:2064–2072. [PubMed: 25046857]
19. Akoum NW, Daccarett M, Wasmund SL, Hamdan MH. An animal model for ectopy-induced cardiomyopathy. Pacing Clin Electrophysiol. 2011; 34:291–295. [PubMed: 21070255]
20. Huizar JF, Kaszala K, Potfay J, Minisi AJ, Lesnefsky EJ, Abbate A, Mezzaroma E, Chen Q, Kukreja RC, Hoke NN, Thacker LR, Ellenbogen K a. Wood M a. Left ventricular systolic dysfunction induced by Ventricular Ectopy: A novel model for premature ventricular contraction-induced cardiomyopathy. Circ Arrhythmia Electrophysiol. 2011; 4:543–549.
21. Wijnmaalen AP, Delgado V, Schalij MJ, van Huls van Taxis CFB, Holman ER, Bax JJ, Zeppenfeld K. Beneficial effects of catheter ablation on left ventricular and right ventricular function in patients with frequent premature ventricular contractions and preserved ejection fraction. Heart. 2010; 96:1275–1280. [PubMed: 20659945]
22. Tan AY, Hu YL, Potfay J, Kaszala K, Howren M, Sima AP, Shultz M, Koneru JN, Ellenbogen KA, Huizar JF. Impact of ventricular ectopic burden in a premature ventricular contraction-induced cardiomyopathy animal model. Hear Rhythm. 2016; 13:755–761.
23. Takada H, Takeuchi S, Ando K, Kaito A, Yoshida S, Hisada S, Mizuno Y. Experimental Studies on Myocardial Contractility and Hemodynamics in Extrasystoles. Jpn Circ J. 1970; 34:419–430. [PubMed: 4102736]

24. Yamaguchi H, Takaki M, Ito H, Tachibana H, Lee S, Suga H. Pressure-interval relationship characterizes left ventricular irregular beat contractilities and their mean level during atrial fibrillation. Jpn J Physiol. 1997; 47:101–110. [PubMed: 9159649]

25. Suzuki S, Araki J, Morita T, Mohri S, Mikane T, Yamaguchi H, Sano S, Ohe T, Hirakawa M, Suga H. Ventricular contractility in atrial fibrillation is predictable by mechanical restitution and potentiation. Am J Physiol. 1998; 275:H1513–1519. [PubMed: 9815055]

26. Tabata T, Grimm R a, Greenberg NL, Agler D a, Mowrey K a, Wallick DW, Zhang Y, Zhuang S, Mazgalev TN, Thomas JD. Assessment of LV systolic function in atrial fibrillation using an index of preceding cardiac cycles. Am J Physiol Heart Circ Physiol. 2001; 281:H573–580. [PubMed: 11454559]

27. Hamlet SM, Wehner GJ, Suever JD, Powell D, Haggerty CM, Jing L, Zhong X, Epstein FH, Fornwalt BK. Effect of variable breath-hold positions during cardiac magnetic resonance on measures of left ventricular mechanics. J Cardiovasc Magn Reson. 2014; 16:P78–P78.

28. Hansen MS, Sørensen TS, Arai AE, Kellman P. Retrospective reconstruction of high temporal resolution cine images from real-time MRI using iterative motion correction. Magn Reson Med. 2012; 68:741–750. [PubMed: 22190255]

29. Feng L, Grimm R, Block KT, Chandarana H, Kim S, Xu J, Axel L, Sodickson DK, Otazo R. Golden-Angle Radial Sparse Parallel MRI: Combination of Compressed Sensing, Parallel Imaging, and Golden-Angle Radial Sampling for Fast and Flexible Dynamic Volumetric MRI. Magn Reson Med. 2013; 717:707–717. [PubMed: 24142845]

30. Otazo R, Candès E, Sodickson DK. Low-Rank and Sparse Matrix Decomposition for Accelerated DCE-MRI with Background and Contrast Separation. ISMRM. 2012; 218:4248.

31. Lustig M, Donoho D, Pauly JM. Sparse MRI: The application of compressed sensing for rapid MR imaging. Magn Reson Med. 2007; 58:1182–1195. [PubMed: 17969013]

WHAT IS KNOWN

- Idiopathic PVCs may create variable symptoms and are thought to cause a cardiomyopathy. Clinically, PVC-induced cardiomyopathy remains a diagnosis of exclusion.
- Conventional imaging is often employed to rule out underlying disease. Techniques such as conventional multi-shot MRI and echocardiography do not provide information regarding the hemodynamic function of different beat types.

WHAT THE STUDY ADDS

- Single-shot 2D MRI, when synchronized with ECG recording, can yield volumetric information regarding different beat types in patients with PVCs.
- The technique demonstrates that patients with similar prevalence of PVC can have different hemodynamic function due to the stroke volume of each beat type as well as the relative prevalence. This approach opens the door for more detailed evaluation of patients with suspected PVC-induced cardiomyopathy.

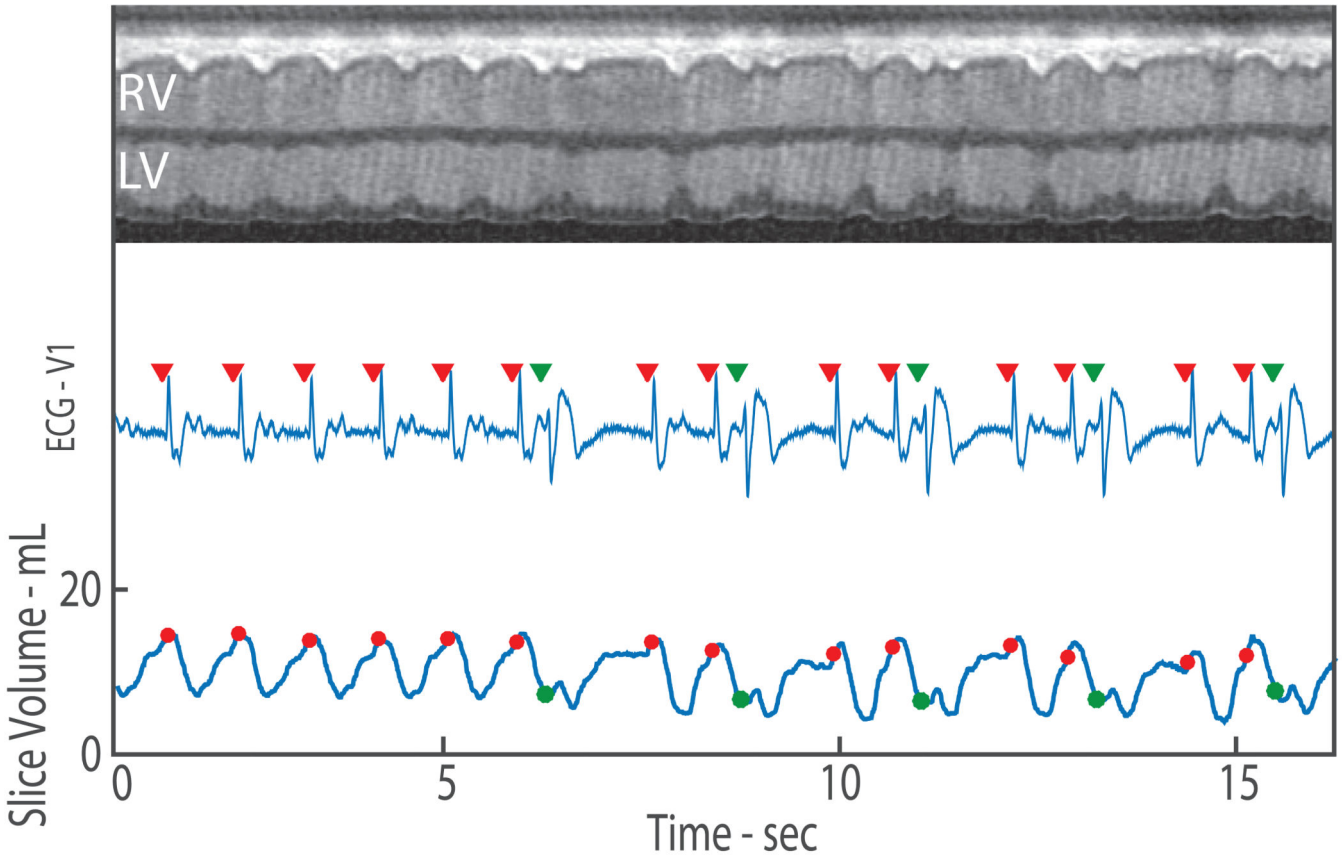

Figure 1.

2D real-time CMR imaging with synchronized ECG recording and measurement of slice volume over time. Top row shows a projection through the heart where the contraction of the left ventricle begins in sinus rhythm and transitions to PVCs. The synchronously recorded ECG is shown in the middle row with the identification of the R-wave demarcated by a red triangle for sinus beats and green triangle for PVC beats. Quantification of slice volume (bottom row) allows for observation of the change in slice function due to arrhythmia. The slice volume associated with the R-wave (beginning of contraction) is shown via dots. For sinus contractions, the red dots occur close to the maximum slice volume (LV EDV). However, during a PVC, the green dots indicate PVC preload which may be substantially lower than the LV EDV.

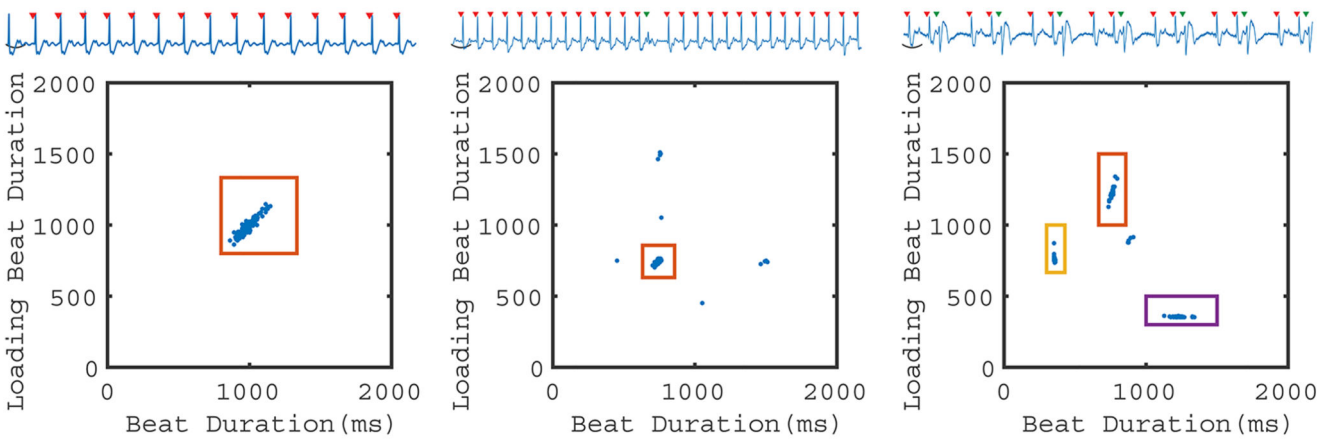

Figure 2.

2D RR-duration plot. Grouping of beat types based on beat duration RR_i and loading (previous) beat duration RR_{i-1}. On the left, a patient with sinus rhythm is shown with a single ECG and one 2D cluster. In the middle, a patient with a single PVC (green triangle) demonstrates how the algorithm can be used to provide arrhythmia rejection. When PVCs are infrequent, they were not observed at all slice locations and therefore did not result in global volume measurements. On the right, a patient in trigeminy exhibits four beat clusters. Three clusters (with colored boxes) were observed at all slice locations. The remaining cluster (sinus-sinus) was only observed at a single slice location and is therefore excluded from further analysis.

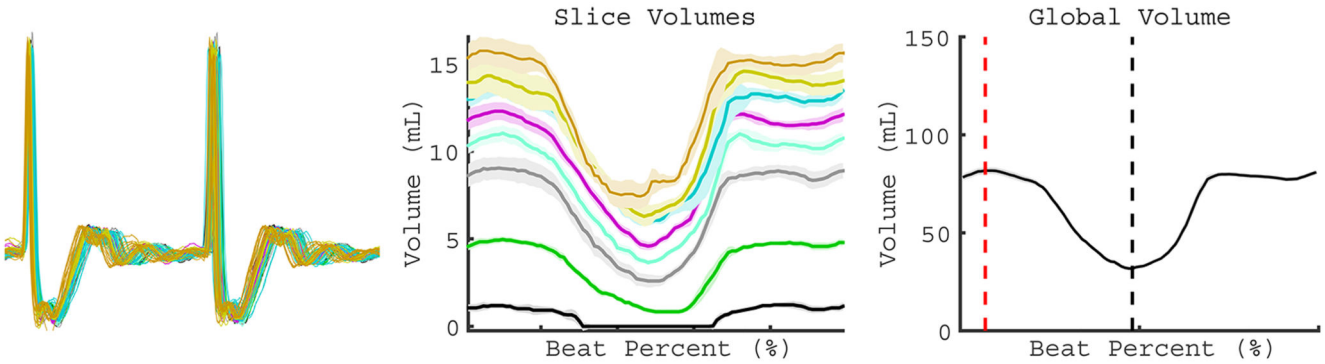

Figure 3.

Global quantification of individual beat types. After definition of a cluster of beats with a similar RR_{i-1} and RR_i, the agreement in recorded ECG over all contractions was visualized (left). Different color volume tracings represent different slices in the short axis of the LV (middle). Summation of 2D slice volume results in global volume (right). After summation, the EDV (vertical red dotted line) and ESV (vertical black dotted line) are determined on the global volume curve (right).

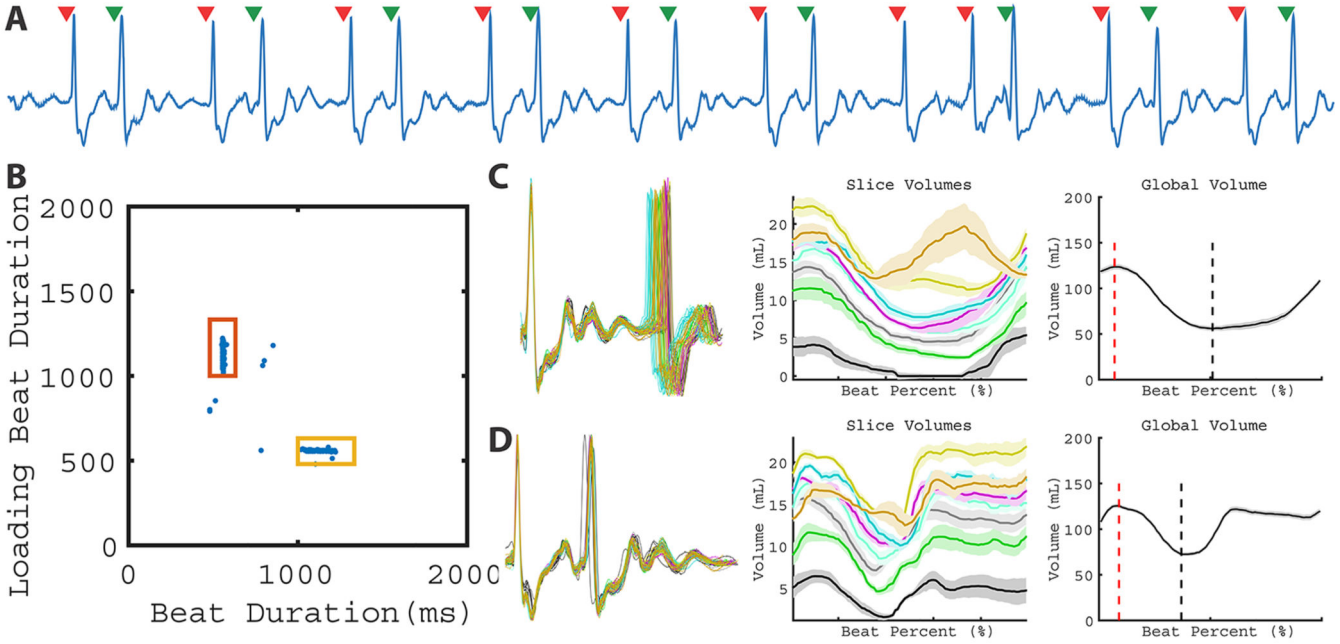

Figure 4.

LV function of a subject with bigeminy. A representative ECG (**A**) from a single slice demonstrates the bigeminy pattern. Two beat clusters are observed in the 2D plot of RR_{i-1} vs RR_i (**B**). As a result, two different global patterns can be quantified in **C** and **D**. Corresponding global volume measurements are found in Table 1 (Patient 6).

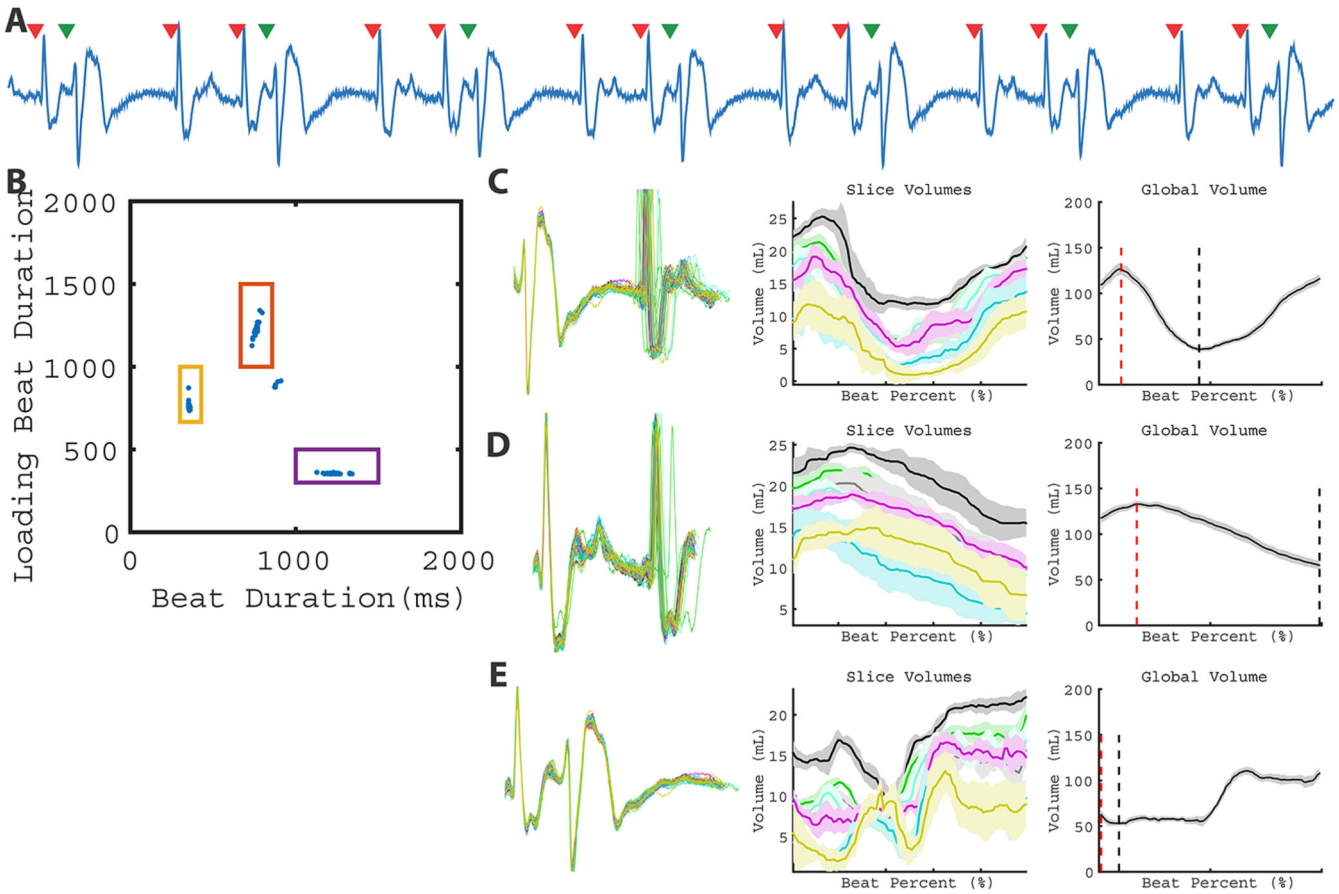

Figure 5.

LV function of a subject with trigeminy. Three types of beats (post-PVC sinus, interrupted sinus, and PVC) can be observed in the ECG (**A**). This leads to three distinct clusters and varying global volume measurements (**B** - **E**). Global volume measurements are found in Table 1 (Patient 7).

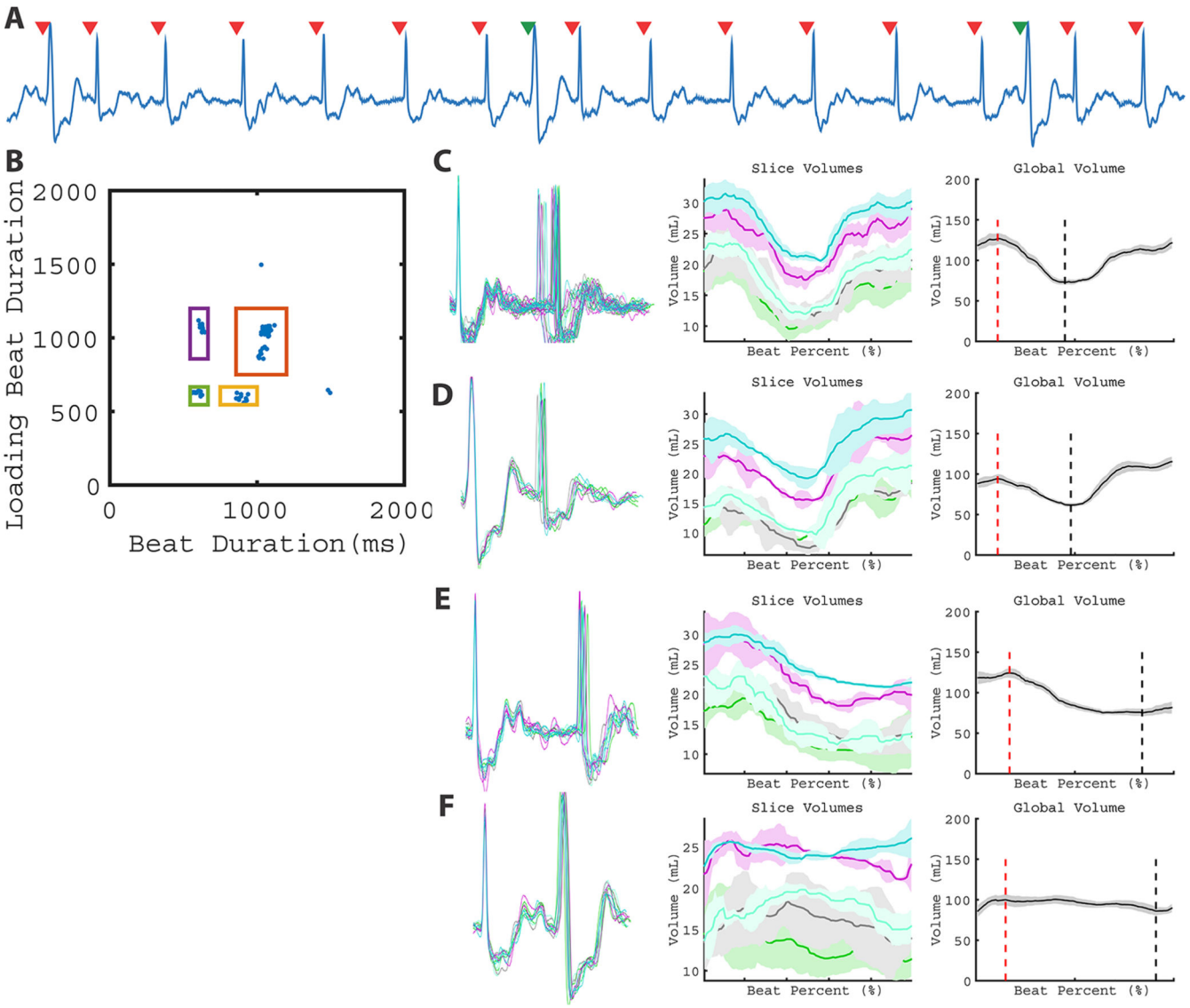

Figure 6.

LV function with interpolated PVCs. The ECG (**A**) and 2D plot (**B**) depict 4 beat types: sinus rhythm (**C**), post-PVC sinus (**D**), interrupted sinus (**E**), and the interpolated PVC contractions (**F**). Global volume quantification suggests interpolated PVCs affect post-PVC loading and do not result in substantial stroke volume. Global volume measurements are found in Table 1 (Patient 8).

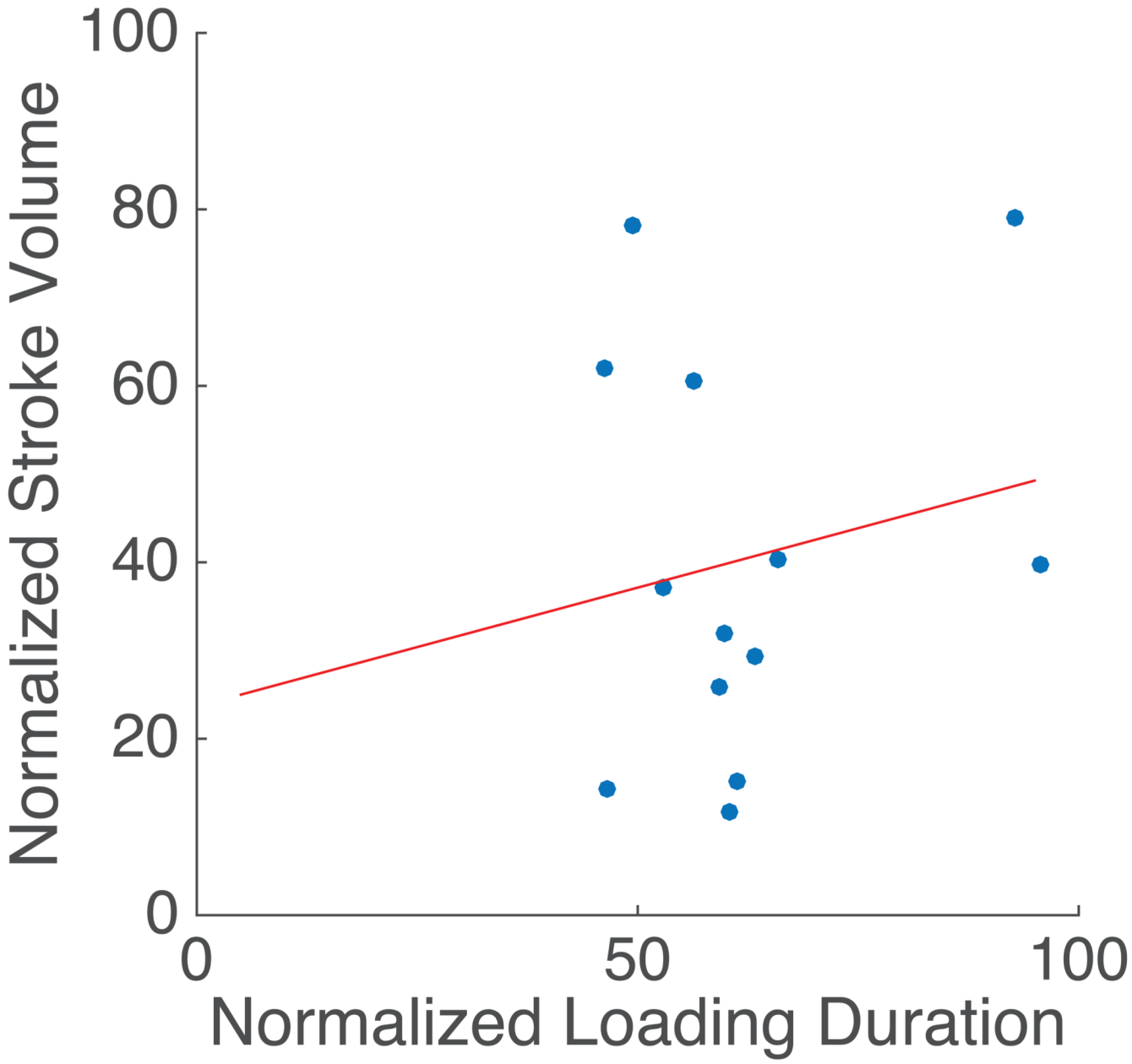

Figure 7.

Normalized stroke volume vs. normalized loading duration. For patients with ectopic contractions, the normalized stroke volume (100 SV_{PVC} / SV_{Sinus}) was plotted as a function of normalized loading duration (100 $RR_{i-1,PVC}$ / $RR_{i-1,Sinus}$). Linear fit: slope = 0.27, y-intercept = 23.6, R^2 = 0.03, p-value = 0.552.

Table 1

Beat characteristics, volumetric measures, and weighted average of study subjects.

Patient Number	Patient Info				Beat Type	Loading Beat Duration (ms)	Beat Observations	Volumetric Measures			Beat Frequency (%)	Temporal Average EF (%)	Echo-Derived EF (%)
	Age	Sex	Arrhythmia Type	PVC Prevalence				V_{max} (mL)	SV (mL)	EF (%)			
1	31	F	History of PVC	0%	Sinus	849.6	207	81.1	44.0	54.3			-
2	22	M	History of PVC	0%	Sinus	905.0	130	143.1	55.2	38.6			38
3	90	F	PVC	4%	Sinus	740.1	20	152.3	59.2	38.9			-
4	56	M	PVC	7%	Sinus	964.0	41	103.5	49.7	48.0			-
5	19	F	Irregular Bigeminy	41%	Post-PVC Sinus	1010.5	66	162.2	59.3	36.5	11	23.0 ± 9.4	36
					PVC	666.3	66	145.6	24.0	16.5	22		
			Post Ablation	8%	Sinus	730.6	66	170.7	60.1	35.2			
6	28	F	Bigeminy	50%	Post-PVC Sinus	1132.6	32	123.7	67.9	54.9	44	48.6 ±6.3	-
					PVC	558.3	53	125.6	53.1	42.3	44		
			PVC	40%	Post-PVC/Sinus	1350.3	51	84.9	52.9	62.2	19	50.1 ± 15.3	-
					Interrupted Sinus	1012.0	41	102.3	63.2	61.8	32		
					PVC	534.1	43	77.4	23.5	30.4	30		
7	51	M	Trigeminy	33%	Post-PVC/Sinus	1224.0	44	126.9	88.2	69.5	29	44.5 ± 22.5	65
					Interrupted Sinus	761.3	39	132.8	67.0	50.5	31		
					PVC	353.9	11	62.5	9.6	15.3	31		
8	58	M	Interpolated PVC	19%	Sinus	1056.3	13	126.8	54.0	42.6	47	36.3 ± 10.1	-
					Post-PVC Sinus	594.1	12	94.4	32.7	34.6	13		
					Interrupted Sinus	1056.3	54	124.3	49.2	39.6	16		
					Interpolated PVC	625.5	18	100.0	14.0	14.0	14		
9	59	F	PVC	35%	Post-PVC/Sinus	1288.6	19	83.9	61.7	73.6	39	69.1 ± 8.8	-
					Interrupted Sinus	1131.4	48	85.5	63.1	73.9	13		
					PVC	675.4	63	38.8	20.2	52.1	14		
10	42	F	Irregular Trigeminy	33%	Post-PVC/Sinus	967.8	38	65.8	42.6	64.8	22	61.7 ± 3.0	62
					Interrupted Sinus	825.2	102	72.5	45.1	62.3	29		
					PVC	766.3	33	62.7	35.6	56.9	18		

Patient Number	Patient Info				Beat Type	Loading Beat Duration (ms)	Beat Observations	Volumetric Measures			Beat Frequency (%)	Temporal Average EF (%)	Echo-Derived EF (%)
	Age	Sex	Arrhythmia Type	PVC Prevalence				V_{max} (mL)	SV (mL)	EF (%)			
11	67	M	PVC	28%	Post-PVC/Sinus	549.4	35	140.6	40.9	29.1	37	27.4 ± 5.2	-
					Interrupted Sinus	736.0	78	149.0	48.6	32.6	12		
					PVC	703.5	56	110.7	19.4	17.5	13		
12	19	M	PVC	25%	Sinus	711.1	58	171.2	64.8	37.9	30	34.5 ± 11.0	-
					Post-PVC Sinus	1103.0	55	149.3	68.6	45.9	22		
					Interrupted Sinus	739.8	36	166.8	62.8	37.7	23		
					PVC	450.8	8	124.4	18.4	14.8	21		
13	56	F	PVC	24%	Sinus	970.6	12	104.9	56.7	54.1	44	54.9 ±5.9	-
					Post-PVC Sinus	1552.2	11	108.3	75.3	69.5	10		
					Interrupted Sinus	970.6	111	122.4	66.6	54.4	15		
					PVC	448.0	15	73.6	35.1	47.7	14		
14	90	M	PVC	14%	Post-PVC/Sinus	1106.2	14	126.6	65.1	51.4	69	47.4 ± 11.9	52
					Interrupted Sinus	936.9	98	127.1	65.5	51.5	9		
					PVC	565.6	19	66.9	7.8	11.6	9		
15	27	F	PVC	13%	Post-PVC/Sinus	1292.5	18	87.2	49.0	56.2	64	50.8 ± 14.5	-
					Interrupted Sinus	977.7	207	99.2	57.5	58.0	12		
					PVC	599.79	130	63.2	8.7	13.8	12		

*EDV: End-diastolic volume,

†stroke volume,

‡EF: ejection fraction,

§PVC: premature ventricular complexes

Table 2

Intra and Interobserver Variability in Measurement of Slice V_{max} and V_{min}.

	Intraobserver		Interobserver	
Cardiac Phase	**CoV (%)**	**Pearson Coefficient**	**CoV (%)**	**Pearson Coefficient**
V_{max}	6.5	0.982	6.4	0.982
V_{min}	8.0	0.988	11.1	0.978